JVC

Journal of Vibration and Control
17(4) 615–622

DOI: 10.1177/1077546310370689
jvc.sagepub.com
SAGE

A new method to predict the permanent deformation of rectangular plates based on shock energy compensation

Liangjun Li and Weikang Jiang

Abstract

The response of plate subjected to underwater explosion loading is of major concern in a variety of marine, ship and offshore platform applications. This paper first conducts the theoretical analysis of the shock loading acting on the plate exposed to underwater explosion. Thereafter, an effective numerical method is adopted to compute the central plastic deformation of the rectangular plates shocked by primary shock wave without regard to the modeling of surrounding water. Therefore numerical computation efficiency is highly improved. Due to the disregard of the gas bubble pulsation energy, numerical central deflections of the rectangular plates are less than the experimental results. Thus, an energy-modified method is advanced to modify the numerical results according to the energy distribution during underwater explosion. The comparison of two types of modified numerical predictions with experimental results piecewise shows good agreement.

Keywords

Air-backed plate (ABP), energy compensation, numerical simulation, permanent deformation, water-backed plate (WBP)

Date received: 25 January 2010; accepted: 30 March 2010

1. Introduction

Plate structures play a key role in a variety of marine, ship and offshore platform applications, and the underwater shock responses of plates have been widely studied to understand the relation between the explosive forces and the plate deformation and fracture behavior. The response of free-standing plates subjected to underwater explosion was investigated by Taylor (1941), Kennard (1944), Cole (1948), Temperley (1950), Keil, (1956, 1961), Ezra (1973), Liu and Yong (2008), Rajendran and Lee (2008), and Rajendran (2009).

Elastic shock response of the air-backed plate (ABP) was presented by Rajendran and Narasimhan (2001) and Hung et al. (2005). Experimental and numerical studies on the plastic deformation of clamped ABPs were performed by many authors (Jiang and Olson, 1996; Rudrapatna et al., 1999; Hammond and Grzebieta, 2000; Ramajeyathilagam et al., 2000; Rajendran and Narasimhan, 2001, 2006; Ramajeyathilagam and Vendhan, 2004; Ashani and Ghamsari, 2008; Rajendran and Lee, 2009). The water-backed plate (WBP) was also researched along with the ABP as it represented the liquid-filled side shell of a ship (Keil, 1956, 1961; Liu and Yong, 2008; Rajendran and Lee, 2008, Rajendran, 2009). Conducting experiments to investigate the dynamic response of plate subjected to underwater explosion is extremely expensive and time-consuming, and environmental protection concerns are another constraint on underwater explosion (UNDEX) testing. In recent decades, numerical methods have been widely used in this area to predict the dynamic response of submerged structures. While the propagation and primary interaction with the target of the shock wave in the water is numerically well established, the contribution due to gas bubble reloading is not usually considered, although the contribution of gas bubble reloading is as much as the primary shock wave itself for a depth explosion that is more than twice the stand off (Rudrapatna et al., 1999).

In the current research, the shock loading acting on the plate subjected to underwater explosion is analyzed

State Key Laboratory of Mechanical System and Vibration, Shanghai Jiaotong University, Shanghai, People's Republic of China

Corresponding Author:
Liangjun Li, State Key Laboratory of Mechanical System and Vibration, Shanghai Jiatong University, Shanghai, People's Republic of China
Email: ljli@sjtu.edu.cn

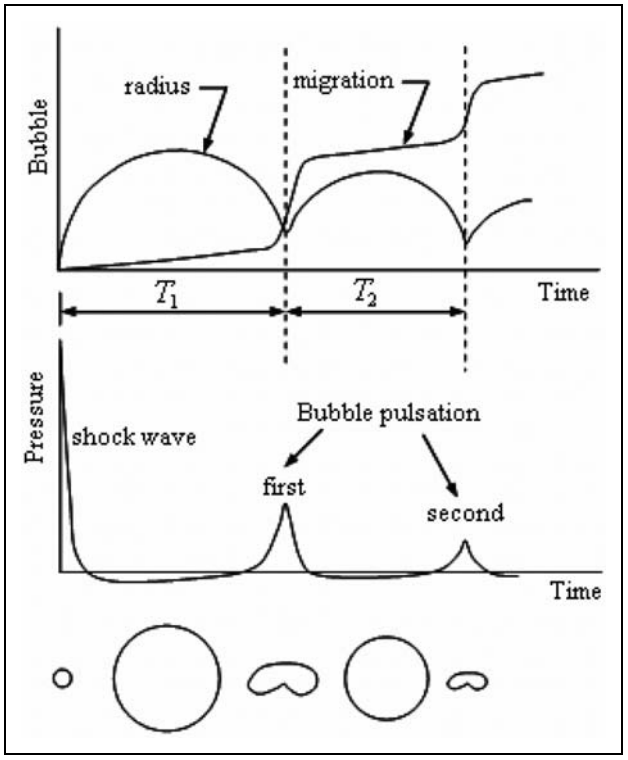

Figure 1. Typical bubble pulsation, migration and free-field pressure history: T_1 and T_2 are the first and second gas bubble pulsating period, respectively.

theoretically based on Taylor's thin plate theory. Thereafter, based on the theoretical analysis, a simplified finite element simulation is brought out to compute the central permanent deformation of the plate duo to the primary underwater shock wave without regard to the modeling of surrounding water. A new energy-modified method is advanced to predict the central plastic deformation of the rectangular plate duo to the shock energy distribution in the underwater explosion, and the comparisons of two types of modified numerical and experimental results are piecewise discussed.

2. Underwater explosion

The sudden energy released associated with the explosion of a high explosive leads to the formation of a superheated, highly compressed gas bubble and generation of a shock wave in the surrounding water (Rajendran and Narasimhan, 2006). The underwater impact wave generated by the explosion is mainly composed of two typical stages: the primary shock wave and the gas bubble pulsating wave illustrated in Figure 1. The primary pressure time history, $P_i(t)$ at a fixed location starts with an instantaneous pressure increase to a peak pressure, P_m, (in less than 10–7 s) followed by a decay which was usually approximated in its initial portion by an exponential function as (Rajendran and Lee, 2009)

$$P_i(t) = P_m e^{-t/\theta} \tag{1}$$

$$P_m = 52.16\left(\frac{W^{1/3}}{S}\right)^{1.13} \tag{2}$$

$$\theta = 96.5(W^{1/3})\left(\frac{W^{1/3}}{S}\right)^{-0.22} \tag{3}$$

$$E_s = \frac{1}{\rho c}\int_0^\infty p_i^2(t)dt = \frac{P_m^2\theta}{2\rho c} \tag{4}$$

Where P_m denotes the peak magnitude of primary pressure in shock front measured in MPa, θ is the time decay constant in micro seconds, E_s is shock energy density of primary shock wave, W is the equivalent quantity of TNT (kg), S is the standoff distance (m), ρ is density of water (kg/m^3), and c is the velocity of sound in water medium (m/s). The gas bubble pulsation wave can be approximately expressed as a normal exponential wave according to the principle of wave profile similitude and the equality of impulses (Liu, 2002)

$$P_g(t) = P_{m1}e^{-(t-T)^2/\theta_1^2} \tag{5}$$

Where P_{m1} and θ_1 are the peak magnitude and time decay constant of the gas bubble pulsation wave, respectively; T denotes the gas bubble pulsation period. For the first gas bubble pulsation wave, θ_1 and T_1 can be calculated by (Liu, 2002)

$$\begin{aligned} \theta_1 &= 20.7\frac{R_0}{P_0^{0.41}} \\ T_1 &= 2.11\frac{W^{1/3}}{(10.3+H)^{5/6}} \end{aligned} \tag{6}$$

Where R_0 is the initial radius of the spherical explosive, P_0 is the hydrostatic pressure of the detonation point in the water, and H is the explosion depth.

As a ship can be subjected to a large variety of underwater explosions, the relation between shock velocity and attack severity is given as the energy density of the shock wave arriving at the ship's hull, which is measured in terms of shock factor η. For normal incidence of shock wave, shock factor η is given as

$$\eta = 0.45\frac{\sqrt{W}}{S} \tag{7}$$

More than half the shock energy released associated with the explosion of a high explosive is dissipated by primary shock wave, and the last is dissipated by the continous gas bubble pulsations. The total shock energy distribution in a free-field underwater explosion is shown in Table 1 (Li et al., 2005).

Table 1. Energy distribution in a free-field underwater explosion.

Underwater explosion loading	Energy consumption (%)	Residual pulsating energy (%)
Primary shock wave	53	47
First pulsating wave	31	16
Second pulsating wave	10	6

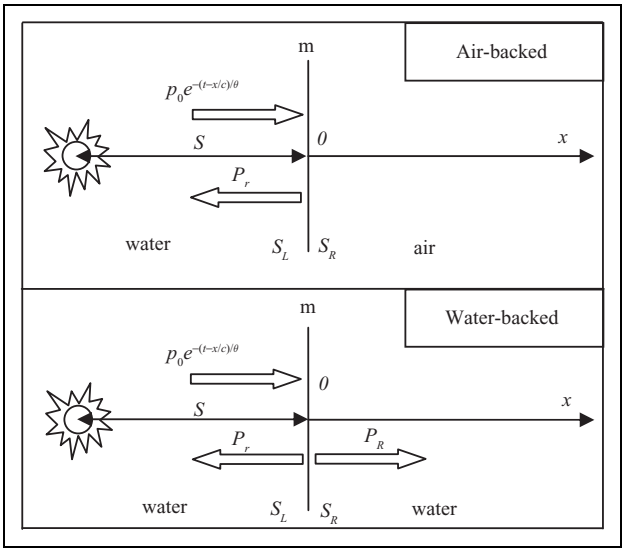

Figure 2. Schematic drawing of the ABP and WBP subjected to underwater explosion.

3. Theoretical analysis for plates under shock loading

3.1. Air-backed plates

A rigid (neglect the elastic, plastic and wave propagation) but free-standing plate of mass per unit area $m = \rho_s h_s$ is considered, where ρ_s and h_s are the density and thickness of the solid plate, respectively. The ABP has only one wetted surface S_L and air on the right side S_R as shown in Figure 2. When the underwater explosion shock wave impinges on the ABP, it gets reflected. The large impedance mismatch between the shock wave and the free-standing plates means that the transmitted part is negligible. The plate subjected to the shock loading starts moving in the x direction with a velocity dx/dt ($v(t)$), where x is the displacement of plate. Equilibrium requirements mean that the water that is in contact with the plates moves along with it, causing a rarefaction pressure component $\rho cv(t)$. The resultant pressure acting on the plate is the sum of contribution of incident, reflected and rarefacted wave pressure. Hence, the governing ordinary differential equation for the motion of ABP as

$$m\dot{v}(t) + \rho cv(t) = 2P_m e^{-t/\theta} \tag{8}$$

For a fixed rigid plate, the incident wave will be fully reflected and the resultant pressure will be doubled on S_L. However, moving the plate in the x direction leads to a partial reflection of incident wave, and the pressure reduction as compared to a fixed plate is $\rho cv(t)$. Applying initial conditions that the displacement and velocity of the plate are zero at time $t = 0$ and introducing the dimensionless inverse mass number $\psi_a = \rho c\theta/m$, the instantaneous velocity of the ABP is given as (Rajendran and Lee, 2009)

$$v(t) = \frac{2P_m\theta}{m(\psi_a - 1)}(e^{-t/\theta} - e^{-\psi_a t/\theta}) \tag{9}$$

and the plate maximum velocity is

$$v_{\max} = \frac{2P_m\theta}{m}\psi_a^{\psi_a/(1-\psi_a)} \tag{10}$$

The pressure acting on S_L of the plate can be obtained by combining equation (8) and (9)

$$P_T(t) = P_L(t) = 2P_m e^{-t/\theta} - \frac{2P_m\psi_a}{(\psi_a - 1)}(e^{-t/\theta} - e^{-\psi_a t/\theta}) \tag{11}$$

As the plate attains its maximum velocity, the hydrostatic pressure of the water in front of it becomes zero and therefore cavitation appears. The time for the plate to reach its maximum velocity or the cavitation time, t_{va}, is given as (Rajendran and Lee, 2008)

$$t_{va} = \frac{\theta \ln \psi_a}{\psi_a - 1} \tag{12}$$

The shock energy transferred to the plate is given as

$$E_{pa} = \frac{1}{2}m\dot{u}_{\max}^2 = \frac{2P_m^2\theta^2}{m}\psi_a^{\frac{2\psi_a}{1-\psi_a}} \tag{13}$$

3.2. Water-backed plate

For a WBP, mass and momentum balance near the right side of the WBP requires

$$v(t) = \frac{P_R(t)}{\rho c} \tag{14}$$

Hence, the equation of motion for the plane can be depicted as

$$m\dot{v}(t) = P_L(t) - P_R(t) \tag{15}$$

Combining equations (14) and (15), the governing ordinary differential equation for the motion of WBP is obtained as

$$m\dot{v}(t) + 2\rho cv(t) = 2P_m e^{-t/\theta} \tag{16}$$

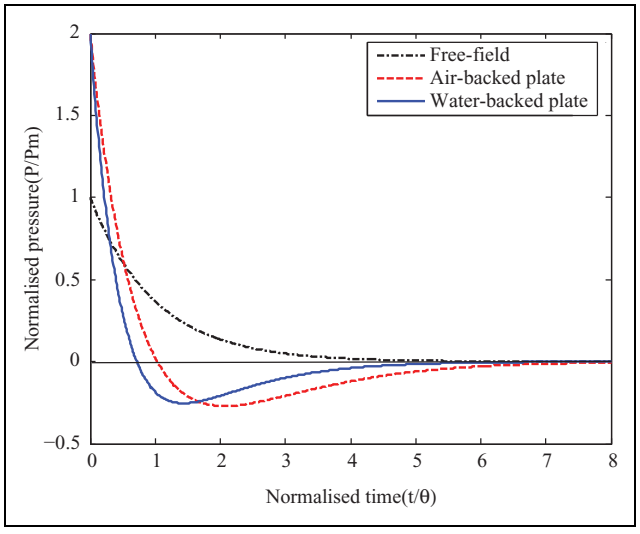

Figure 3. Variation of normalized pressure on the plate (with respect to shock wave peak pressure) with normalized time.

Applying initial conditions that the displacement and velocity of the plate are zero at time $t = 0$ to solve the plate displacement from equation (16) (Rajendran and Lee, 2008)

$$v(t) = \frac{2P_m\theta}{m(\psi_w - 1)}(e^{-t/\theta} - e^{-\psi_w t/\theta}) \tag{17}$$

Where $\psi_w = 2\rho c\theta/m$ is the dimensionless inverse mass number for WBP. Notice that $\psi_w = 2\psi_a$, as defined above. Hence, forms of the theoretical results for WBP are the same as that for ABP. The results are summarized below for the comparison with the ABP solution. For the presentation hereafter, superscripts w will be used to represent WBP (Rajendran and Lee, 2008).

$$v^w_{\max} = \frac{2P_m\theta}{m}\psi_w^{\psi_w/(1-\psi_w)} \tag{18}$$

$$P^w_L(t) = 2P_m e^{-t/\theta} - \frac{P_m\psi_w}{(\psi_w - 1)}(e^{-t/\theta} - e^{-\psi_w t/\theta}) \tag{19}$$

$$P^w_R(t) = \frac{P_m\psi_w}{(\psi_w - 1)}(e^{-t/\theta} - e^{-\psi_w t/\theta}) \tag{20}$$

$$P^w_T(t) = 2P_m e^{-t/\theta} - \frac{2P_m\psi_w}{(\psi_w - 1)}(e^{-t/\theta} - e^{-\psi_w t/\theta}) \tag{21}$$

$$E_{pw} = \frac{1}{2}mv^w_{\max^2} = \frac{2P_m^2\theta^2}{m}\psi_w^{\frac{2\psi_w}{1-\psi_w}} \tag{22}$$

$$t_{va} = \frac{\theta \ln \psi_w}{\psi_w - 1} \tag{23}$$

The theoretical shock pressures acting on the plate are shown in Figure 3.

4. Underwater explosion experiments

The detailed procedure that was employed for carrying out plastic experiments of the plates was depicted in Rajendran and Narasimhan, (2001). However, for the sake of completion, a few of the salient details are presented here. All the underwater explosion experiments were performed in a shock tank (15 m × 12 m × 10 m), and the experiment setup was immersed to a depth of 2 m. This ensured that the effect of reflected wave from the tank walls was insignificant. In all the experiments, the explosive was placed on the normal line passing through the centre of the plate and the stand off was 0.15 m, which was less than half the depth of the explosion. This ensured that the gas bubble reloading effects were maximum for the plastic experiments. Test plate dimensions were such that the diffraction time (83 μs) was much larger than the shock wave time constant so that the effect of the primary shock pulse was fully felt by the exposed area of the test plate. Rectangular thin plates were 0.55 m × 0.45 m × 0.004 m in size with an exposed area of 0.30 m × 0.25 m. The characteristics of underwater explosion loading and experiment results are presented in Table 2.

5. Numerical simulation

5.1. Finite element modeling

The finite element package ABAQUS/Explicit is used for carrying out the numerical simulation of the rectangular plates subjected to underwater explosion. During the traditional finite element simulations, the structure domain is modeled by the structure element and water surrounding the plate is modeled by an acoustic element which has much more elements than the structure. The fluid-structure interaction is also modeled which will greatly increase in computing resources. This paper adopts a simple numerical method to investigate the elastic-plastic deformation of the rectangular plates subjected to primary shock wave. During the simulation, only the plate is modeled in order to save computing resources.

The rectangular plate is modeled using four-node shell elements available in ABAQUS finite-element software. Clamped edge condition is assumed and only one-fourth of the plate is considered for the analysis because of symmetry as shown in Figure 4. Before the plastic deformation simulation, the mode analysis of the rectangular plate which is under investigation by block Lanczos mode extraction method yields the three modes of natural frequencies. The underwater explosion loading ignoring the gas bubble reloading acting on the plate has been estimated as discussed in section 3 and compiled as a load subroutine VDLOAD. During the numerical simulation, VDLOAD is called and applied force is

Table 2. Summary of results of plastic deformation experiments, stand off = 15 cm.

Sl. no.	Charge weight W (g)	Shock factor $(0.45\times W^{1/2}/R)$	Time decay constant θ (μs)	Time decay constant θ_1 (μs)	Permanent deformation of ABP (mm)
1	5	0.212	16.7	1626	12
2	10	0.300	20.0	2048	23
3	15	0.367	22.2	2345	27
4	20	0.424	23.9	2581	32
5	30	0.520	26.6	2955	42
6	40	0.600	28.7	3252	50
7	50	0.671	30.4	3503	58
8	60	0.735	31.9	3723	65
9	70	0.794	33.2	3919	72
10	80	0.849	34.3	4097	Rupture

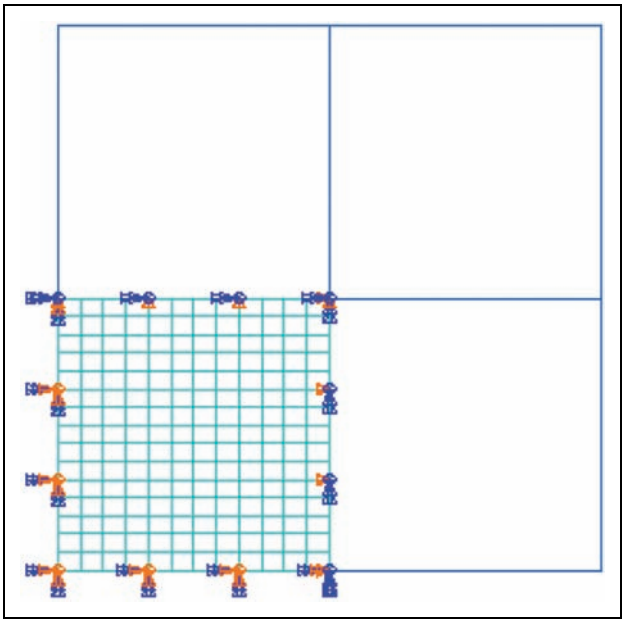

Figure 4. Finite-element model of the rectangular plate.

computed according to the instantaneous information of plate nodes in every time increment.

5.2. Material model

The uni-aixal strain-stress properties obtained for the HS steel have been used as the primary material data. The constitutive model selected for the nonlinear analysis is the elasto-plastic material model with isotropic hardening. In order to include the effect of strain rate in the finite element analysis, the Cowper-Symonds model is used to calculate the dynamic yield stress.

$$\sigma_{dy} = \sigma_y \left(1 + \left|\frac{\dot{\varepsilon}}{D}\right|^{1/n}\right) \tag{24}$$

Table 3. Natural frequencies of the rectangular thin plate.

Mode orders	1	2	3
Frequencies (Hz)	491	887	1104

6. Results and discussion

6.1. Numerical permanent deformation prediction of air-backed plate

The first three natural frequencies of the rectangular plate are shown in Table 3 and the basic frequency of the underwater explosion loading can be calculated according to inversing the time decay constant θ_1. The numerical central permanent deformations are shown in Table 4 and the comparison of the numerical results with experiments is depicted in Figure 5. It can be concluded that the experimental central plastic deformations are linear increasing to the shock factor except the second value, because the basic frequency (488.3 Hz) of the gas bubble pulsation reloading in the second experiment is adjacent to the first mode of natural frequency as 491 Hz, so that the central plastic deformation of the plate is enlarged.

The gap between the numerical and experimental results is gradually increasing along with the increasing of shock factors. During the underwater explosion, both the primary shock wave and the partial gas bubble reloading contribute to the central deformation of the rectangular plate. When the shock factor is rather small, the first gas bubble pulsating reloading partially contributes to the permanent deformation, so the numerical permanent deformation of the plate is just a little less than the test result. Accompanying the increasing of the shock factor, even both all the first and partial the second gas pulsating reloading contributes to the central permanent deformation of plate, and the numerical deformation is much less than the experimental deformation as shown in Figure 5.

Table 4. Summary results of central plastic deformation of plates, stand off =15cm.

Sl. no.	Charge weight W (g)	Shock factor ($0.45 \times W^{1/2}/R$)	Numerical permanent deformation of ABP(mm)	Numerical permanent deformation of WBP(mm)
1	5	0.212	9.5	6.4
2	10	0.300	14.9	9.5
3	15	0.367	18.6	12.0
4	20	0.424	21.5	14.1
5	30	0.520	26.5	17.2
6	40	0.600	30.7	19.8
7	50	0.671	34.4	22.0
8	60	0.735	37.7	24.1
9	70	0.794	40.6	26.0

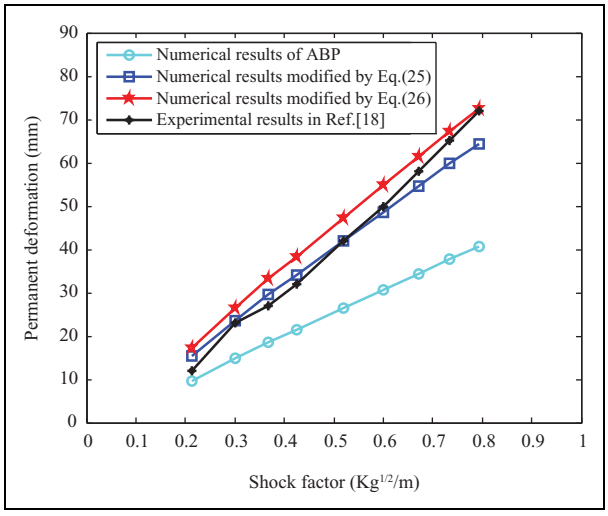

Figure 5. Comparison of numerical and experimental plastic deformations of ABP.

Considering the contribution of gas bubble pulsating reloading to the plate central deformation, the numerical results based on the primary shock wave must be modified. When the plate subjects to the underwater explosion, shock energy is transmitted to the plate and deformation occurs. If the underwater explosion is rather intensive, the energy of the gas bubble pulsating transmitted to plate cannot be ignored. According to the energy distribution in underwater explosion shown in Table 1, the numerical central permanent deformation must be modified by multiplying a scale factor ζ which reflects the gas bubble pulsation energy transmitting to the plate. When the plastic deformation of the rectangular plate occurs, the material is in plastic flow phase and the mean equivalent stress remains practically unchanged. The plastic deformation due to the energy transmitted to the plate is assumed to be linear to the energy distributed in the primary shock wave and gas bubble pulsating wave.

If only the first gas bubble pulsation energy contributes to the plate deformation, the relationship between numerical and modified numerical permanent deformation can be expressed as

$$\delta_m = \zeta\delta = \left(1 + \frac{31\%}{53\%}\right)\delta \tag{25}$$

Where, δ and δ_m are numerical and modified numerical central permanent deformation of the rectangular plate, respectively. If all the first and second gas bubble pulsating energy is assumed to contribute to the plate central deformation, the relationship between numerical and modified numerical central permanent deformation can be expressed as

$$\delta_m = \zeta\delta = \left(1 + \frac{31\%}{53\%}\right)\left(1 + \frac{10\%}{53\% + 31\%}\right)\delta \tag{26}$$

The comparisons of modified numerical permanent deformation and experimental results are also shown in Figure 5.It can be observed from Figure 5 that the modified numerical central permanent deformation is much large than that of the experiment when the shock factor is less than 0.3, because little gas bubble pulsation reloading contributes to the plastic deformation of plate. The numerical central permanent deformation modified by equation (25) shows good agreement with that of the experiment when the shock factor is between 0.3 and 0.67. While the numerical results modified by equation (26) are in good agreement with experiments when the shock factor is larger than 0.67 and two data lines meet with each other at last.

6.2. Numerical permanent deformation prediction of water-backed plate

The numerical central permanent deformation comparisons of water-backed with ABPs are shown in Table 4. It can be concluded that the ratios of central permanent deformation of water-backed to ABPs almost remain constant as depicted in Figure 6. So, it is available to predict the central permanent deformation of WBP based on the response of the same ABP subjected to underwater explosion. The numerical results of WBPs are also needed to modify by

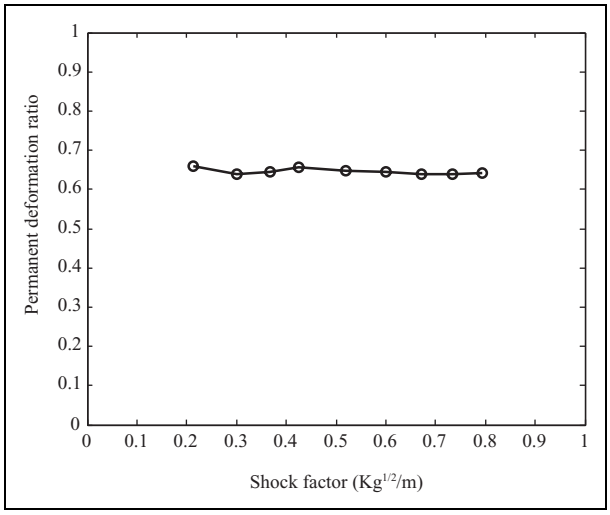

Figure 6. Numerical permanent deformation ratio of water-backed and ABP.

equations (25) and (26) to predict the actual plastic deformations based on the same energy-modified theory.

7. Conclusions

In this paper, a new effective finite element method based on primary shock wave is adopted to predict the central permanent deformation of rectangular plates subjected to underwater explosion to compare against the published results. Without gas bubble pulsation reloading consideration, the numerical central plastic deformations of plate differ largely with the experimental observations. So, an effective modified method are advanced based on the energy distribution in underwater explosion to revise the numerical results, and two types of the modified results piecewise show good agreements with the experimental results in Rajendran and Narasimhan (2001). The almost constant permanent deformation ratio of water-backed to ABPs is also concluded, which can be used to predict the central plastic deformation of WBPs.

References

Ashani, J. Z. and Ghamsari, A. K., 2008, "Theoretical and experimental analysis of plastic response of isotropic circular plates subjected to underwater explosion loading," *InterScience* **39**, 171–175.

Cole, R. H., 1948, *Underwater Explosions [M]*, Princeton University Press, New Jersey.

Ezra, A .A., 1973, *Principles and Practice of Explosive Metalworking*, vol. 1., Industrial Newspapers Ltd., New York.

Hammond, L. and Grzebieta, R., 2000, "Structural response of submerged air-backed plates by experimental and numerical analyses," *Shock and Vibration* **7(6)**, 333–341.

Hung, C. F., Hsu, P.Y., and Fuu, J. J. H., 2005, "Elastic shock response of an air-backed plate to underwater explosion," *International Journal of Impact Engineering* **31**, 151–168.

Jiang, J. and Olson, M. D., 1996, "Non-linear transient analysis of submerged circular plates subjected to underwater explosions," *Computer Methods in Applied Mechanics and Engineering* **134**, 163–179.

Keil, A. H., 1956, *Introduction to Underwater Explosion Research*, Underwater Explosions Research Division (UERD), Norfolk Naval Ship Yard, Portsmouth, Virginia.

Keil, A. H., 1961, "The response of ships to underwater explosions," *Transactions of the Society of Naval Architects and Marine Engineers* **69**, 366–410.

Kennard, A. H., 1944, "The effect of pressure wave on a plate or diaphragm," *Compendium of Underwater Explosion Research* **3**, 11–64.

Li, G., Li, Y., and Zhang, X., 2005, "Experimental verification of relationship between bubble motion and shock vibration of ship equipment," *Journal of Ship Mechanics* **9(1)**, 98–105.

Liu, J., 2002, *Theory and its Applications of Ship Dynamic Responses to Un-contact Underwater Explosions [D]*, China Ship Scientific Research Center, Wuhan, People's Republic of China.

Liu, Z. and Yong, Y. L., 2008, "Transient response of submerged plates subjected to underwater shock loading: an analytical perspective," *Journal of Applied Mechanics* **75**, 044504–1–044504–5.

Rajendran, R., 2009, "Effective shock factors for the inelastic damage prediction of clamped plates subjected to non-contact underwater explosion," *Journal of Strain Analysis* **44**, 211–219.

Rajendran, R. and Lee, J. M. A., 2008, "Comparative damage study of air- and water-backed plates subjected to non-contact underwater explosion," *International Journal of Modern Physics B* **22(9–11)**, 1311–1318.

Rajendran, R. and Lee, J. M., 2009, "Blast loaded plates," *Marine Structures* **22**, 99–127.

Rajendran, R. and Narasimhan, K., 2001, "Linear elastic shock response of plates subjected to underwater explosion," *International Journal of Impact Engineering* **25**, 493–506.

Rajendran, R. and Narasimhan, K., 2001, "Performance evaluation of HSLA steel subjected to underwater explosion," *Journal of Materials Engineering and Performance* **10**, 66–74.

Rajendran, R. and Narasimhan, K., 2006, "Deformation and fracture behavior of plate specimens subjected to underwater explosion - a review," *International Journal of Impact Engineering* **32**, 1945–1963.

Ramajeyathilagam, K. and Vendhan, C. P., 2004, "Deformation and rupture of thin rectangular plates subjected to underwater shock," *International Journal of Impact Engineering*," **30**, 699–719.

Ramajeyathilagam, K., Vendhan, C. P., and Bhujanga Rao, V., 2000, "Non-linear transient dynamic response of rectangular plates under shock loading," *International Journal of Impact Engineering* **24**, 999–1015.

Rudrapatna, N. S., Vaziri, R., and Olson, M. D., 1999, "Deformation and failure of blast-loaded square plates," *International Journal of Impact Engineering* **22**, 449–467.

Taylor G. I., 1941, "The pressure and impulse of submarine explosion waves on plates," *Compendium of Underwater Explosion Research* **1**, 1155–1174.

Temperley, H. N. V., 1950, "Theoretical investigation of cavitations phenomena occurring when an underwater pressure pulse is incident on a yielding surface," *Compendium of Underwater Explosion Research* **3**, 260–268.